

Master in Photonics

MASTER THESIS WORK

Multifunction LED lighting system combining tunable spectrum and data communication

Alonso Rodríguez Trujillo

Supervised by Dr./Prof. María S. Millán García-Varela, (UPC) and
Dr. Jorge E. Higuera Portilla, (IREC)

Presented on date 8th September 2015

Registered at

ETSEIB Escola Tècnica Superior
d'Enginyeria de Telecomunicació de Barcelona

Multifunction LED lighting system combining tunable spectrum and data communication

Alonso Rodríguez Trujillo

Smart Lighting Laboratory, Lighting Group, Institut de Recerca en Energía de Catalunya (IREC), Jardins de les Donde de Negre N^o1, 2nd floor, 08930, Sant Adrià de Besòs, Barcelona, Catalonia, Spain.

E-mail: alonsotruetz@gmail.com

Abstract. In this project a novel portable Visible Light Communication (VLC) system comprising an inexpensive and easy to fabricate multi-channel transmitter (Tx) and a receiver (Rx) have been developed. The light engine is designed to support up to three different LED channels while illuminating an indoor space changing the spectrum according to human circadian rhythms or any other desires. The Tx module architecture contains a programmable microcontroller and a constant current LED driver to manage the data to be transmitted. The Rx module allows the detection of optical signals, decoding and recovering the complete information with a circuit containing three stages: transimpedance amplifier, serializer and deserializer stages, controlled by a microcontroller unit. The VLC link has been tested in a laboratory environment with natural illumination to operate for distances up to 8 meters (at 700 kbps), data rates up to 4.50 Mbps (at 2 meters), and angles up to 75° (at 700 kbps and 2 meters). Under these conditions the flickering effect is completely removed.

Keywords: Visible Light Communications (VLC), Smart Lighting, Light Emitting Diodes (LEDs), Optical Wireless Communications, Quality Factor (Q), Bit Error Rate (BER), Flickering effect.

I. Introduction

Digital light is a concept that involves illumination with Solid State Lighting (SSL) technologies [1] such as light emitting diodes (LEDs) and/or organic light emitting diodes (OLEDs) with additional communications capabilities and different wired or wireless communications interfaces (DALI, DMX, Wi-Fi, Bluetooth, ZigBee and VLC among others). The current development of SSL technology for illumination, shows a high advantage with respect to conventional lighting technologies. In this context, modern light engines consume less energy than traditional lighting sources (incandescent bulbs, halogen lamps, mercury vapour lamps and fluorescent tubes). At present, the efficacy in LEDs is higher than 150 lm/W. Also, LEDs have a long life (more than 100.000 hours) and emitters can be spectrally tunable sources (which allows for an easily colour mixing and dynamic colour reproduction in real time). In addition, LEDs are inexpensive, easy to fabricate and may be modulated at very high speeds in the range of several MHz, which gives a chance for further applications in optical communications [2] or Human Centric Lighting (HCL), and not only for general lighting or signalling applications.

The concept of Visible Light Communications (VLC), (called Li-Fi when is bidirectional), concerns the technology aiming to transmit data while providing light for illumination [3], and it usually uses LEDs to do so. It means that the data is encoded in the visible light ($380\text{ nm} \leq \lambda \leq 780\text{ nm}$) transmitted by those LEDs, and the simplest way to do it is through the digital modulation methods. The fact that it uses visible light is an advantage regarding the lack of licence requirements for its use, the low interferences, and the high security it presents thanks to the fact that visible light does not crosses the walls (moreover, synchronization between the luminaries in a building may be achieved in order to allow a data transmission even if the receiving gadgets are moving from one place to another).

White light is always used for lighting applications. That is why most of the research in VLC use LED solutions providing white light, but there are three different ways to provide white light using LEDs: RGB LEDs, PC-LEDs and OLEDs. Table 1 summarizes the main features

and fundamentals [1] of current state-of-the-art LEDs and provides information related to the biggest breakthroughs on each technology.

Table 1. LEDs providing white light: Fundamentals and state of the art.

Fundamental	Number of Channels	Achievement	Additional features	Ref.		
RGB LED: Three different inorganic LEDs (red, green and blue) emit jointly white light on average. The relative intensity of each LED gives rise to different kinds of white (cold, neutral, warm...)	3	3.4 Gbps at 10 cm	Equalization	[4]		
		3 Gbps at 5 cm	Equalization	[5]		
		3.22 Gbps at 25 cm		[6]		
		575 Mbps at 66 cm		[7]		
		477 Mbps at 40 cm		[8]		
		1.25 Gbps at 10 cm		[9]		
		2.1 Gbps at 10 cm	Optimum power	[10]		
		1.1 Gbps at 1 m	Multiple Input Multiple Output (MIMO) system	[11]		
		1 Gbps at 50 cm		[12]		
		340 Mbps at 43 cm	Post-equalization	[13]		
Phosphorous Coating LED (PC-LED): An inorganic blue LED made of InGaN with a phosphorous coating made of YAG which absorbs blue photons exciting electrons to upper orbitals from which they decay later in several steps emitting less energetic photons ranged over a wide spectrum giving rise to a (either cold, or neutral, or warm...) white averaged emission	1	150 Mbps at 50 cm	Neural network	[14]		
		10 Mbps at 1 m	Non-Return to Zero Inverted (NRZI)	[15]		
		3.4 Mbps at 80 cm		[16]		
		2 Mbps at 40 cm		[17]		
		220 Mbps at 1 m	MIMO system	[18]		
		OLED: Organic LED emitting photons at different energy levels so that it gives rise to an averaged white light	1	2.7 Mbps at 10 cm		[19]
				1.4 Mbps at 30 cm		[20]

To the best of our knowledge, currently, VLC systems lack of important features such as extended coverage ranges (distance), wide aperture angles for light collection, low cost, spectrally-tunable capabilities of the light source and portability of the source and receiver. Therefore, in this work we investigate how these additional features could be included in the next generation of VLC systems with reduction of annoying side effect. In this sense we aim to **avoid flickering effects** (light intensity changes when sending alternating ones and zeroes which may cause health troubles as headaches) by increasing the data rate over a certain acceptable limit, **supporting an average constant intensity** for lighting comfort purposes in Human Centric Applications (HCA), using **low cost and portable hardware** architectures, providing **spectrum tunability**, and **achieving practical results in distance, speed and aperture (angle)**.

In all cases, we try to improve the range of detection indoors using an inexpensive setup for practical purposes. In this case, much humbler data rates have been achieved but getting practical application in real cases.

In order to develop the different experiments, three different kinds of white LEDs of different Colour Correlated Temperatures (CCT) and another three Red (R), Green (G) and Blue (B) colour LEDs have been used. This hardware setup allows the possibility for implementing a spectrally tunable VLC system that changes its spectral content in a room according to HCL objectives.

The idea of this election has the purpose to offer two different solutions: In the first case it is possible to use red, green and blue LEDs giving rise to different averaged whites (metamers) depending on the relative light intensity of every channel (flexible tunability) while emitting information through three different channels (for which it would be required to have got three different receivers plus filters in order to take advantage of the whole potential this system has got); and in the second one it is possible to use three different preselected kinds of white light

(hot, neutral and cold) for three different environments very easily interchangeable emitting just in one channel at a time. The latter has the advantage that it is easier to manage the light environment but it also has the drawbacks that it emits through just one channel instead of three and the provided environments are less flexible. The operational procedure requires programming different firmwares in both Tx and Rx modules to send and receive information.

Section II includes a more detailed description of the hardware used in this project; section III gives some theoretical background for the metrics of Bit Error Rate (BER) and Quality Factor (Q) on which our communication quality measurements are based; then, the results are presented and discussed in section IV; and finally, in section V the main conclusions are outlined.

II. Hardware Architecture

The prototype consists of two parts: A transmitter (Tx) and a receiver (Rx). At the same time, each part consists of several sub-modules. The whole setup schematic is represented in figure 1.

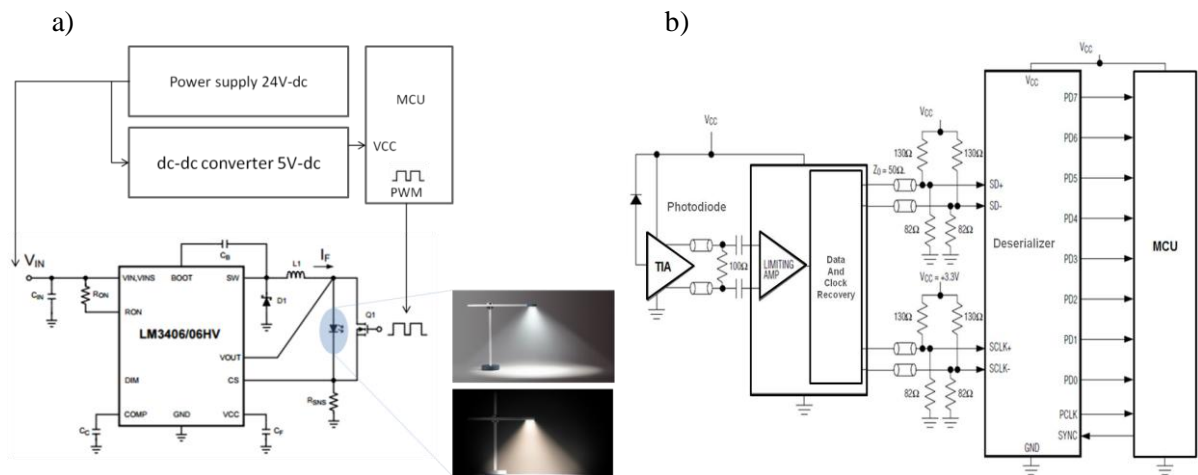


Figure 1. Schematic of the setup: (a) a transmitter made out of a 24 V supply, a dc-dc converter, a microcontroller (MCU), a MOSFET (Q1), a driver (LM3406HV) and external LEDs (in fact there are three channels, every one made out of a MOSFET, a driver and an LED array); and (b) a receiver made out of a silicon photodiode, a transimpedance amplifier (TIA), a low pass filter, a clock recovery and data retiming (containing a previous limiting amplifier), a deserializer and a microcontroller (MCU).



Figure 2. Picture of the transmitter: (a) Top view of the circuit made out of a 24 V supply and a dc-dc converter stage (red ellipse) with the dc-dc converter chip (orange ellipse), a microcontroller (blue rectangle) and three channels (green polygons) in which there are two different eligible MOSFETs (violet ellipse), a driver (yellow circle) and a connector (brown rectangle) for the external LEDs; and (b) a picture of the whole transmitter formed by the circuit and the external LEDs connected (in this case to channel number 2).

In the case of the transmitter (Tx) (see figure 1 (a) and figure 2), it contains an electronic circuit and some easily interchangeable arrays of LEDs externally coupled to this circuit. At the same time, the Tx module consists of three parts: A dc-dc converter from 24 V (power supply) to 5 V; an MBED microcontroller (MCU) fed with those 5 V which will control the performance of the data transmission according to a certain firmware designed to transmit information at will in the form of “ones” and “zeroes”; and three different channels connected to the external LEDs. And,

finally, at the same time, every one of those three channels is formed by another three components: A fast MOSFET to control when the current may flow through the external LEDs; a driver, which is useful to produce a roughly constant current source of 350 mA to feed the LEDs when the MOSFET allows it; and some complementary to the driver passive components (resistors, capacitors and inductors). Indeed, in figure 2 it may be seen that, in fact, there are two MOSFETs per channel. Only one of them is working at a time, and it may be selected by the position of adjacent “jumpers”.

In the case of the receiver (Rx) (see figure 1(b) and figure 3), it consists of five parts: A silicon photodiode to convert photons into current; a transimpedance amplifier (TIA) in order to convert the input current signal into an output voltage drop signal, plus low pass filters to clean the signal from noise; a clock-recovery and data retiming to transmit the received signal in serial mode; a 1:8 Deserializer to recover the information in parallel, and also improves again the signal digitalizing it; and another microcontroller in order to receive and decode the parallelized information.

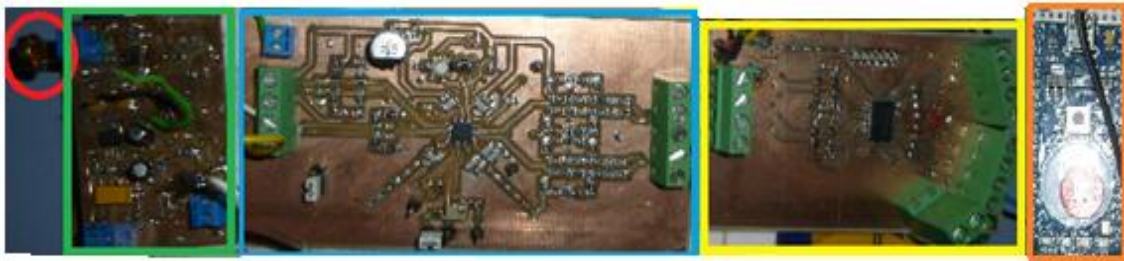


Figure 3. Picture of the receiver: There is a photodiode (red ellipse), a Transimpedance Amplifier (TIA) stage (green rectangle), a Clock Recovery and Data Retiming stage (blue rectangle), a Deserializer stage (yellow rectangle) and a microcontroller (orange rectangle).

2.1. Transmitter characteristics

In order to manage all LED channels covering different colours independently, we have worked with different LED types as shown in table 2.

Table 2. LEDs under test.

	LED1	LED2	LED3	LED4	LED5	LED6
Model	OSRAM Dragon ILS-GD06-RED1-SD101	Philips Lumileds Rebel LXML-PM01-0090-CT1/N4B	Philips Lumileds Rebel LXML-PB01-0030-3-CT/F3C & LXML-PR01-0500-CT/F5C	OSRAM Dragon ILS-GD06-HWWH-SD101	OSRAM Dragon ILS-GD06-NWWH-SD101	Beijing Yuji LDM-6200
Colour	Red	Green	Blue	Hot White	Neutral White	Cool White
Peak wavelength, λ (nm)	623.7	536.1	464.7	582.9	576.4	472.1
Colour Temperature, T (K) (and CRI)	-	-	-	2746 (82.0)	3938 (84.0)	6233 (94.1)
CIE 1931 chromaticity coordinates (x, y)	(0.6838, 0.3029)	(0.2286, 0.6844)	(0.1486, 0.0582)	(0.4631, 0.4218)	(0.3880, 0.3959)	(0.3190, 0.3159)
E_e (W/m²) at 50 cm	2.971	0.5799	1.661	7.566	3.901	0.8934
E (Lm/m²) at 50 cm	575.8	283.8	94.15	2417	1244	248.1

Figure 4 depicts the chromatic coordinates of the LEDs used in this work on a standard CIE1931 chromaticity diagram. We remark that our LEDs were not very intense. As a matter of fact, their power was not enough for a proper illumination, with at least 500 lx (according to the ISO 12464-1 standard), of a table placed at two meters from the ceiling.

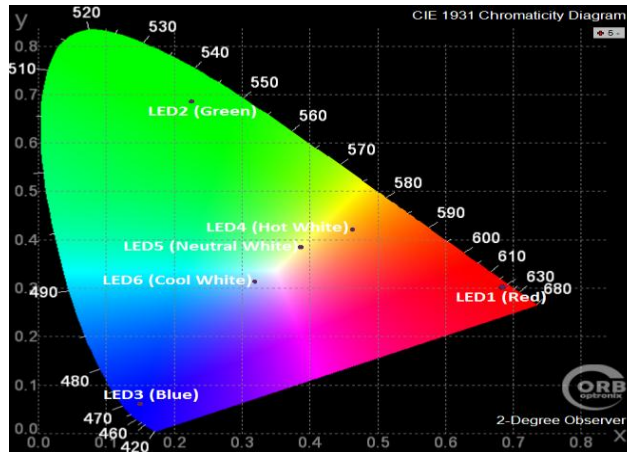


Figure 4. CIE 1931 Chromaticity diagram with the points corresponding to the 6 LEDs emitters used in the prototype.

LEDs are inherently current-driven devices. The datasheet of each LED should specify the current under which they work with highest performances. For most cases, high brightness LEDs are designed to work at 350 mA, as in the case of the LEDs chosen for this project. For this reason it is important to provide some constant current source to feed the LEDs at that specific current. In this case, a driver (LM3406HV) is configured as a constant-current buck regulator. The LM3406HV model is simple to configure as a current source and uses few external components including an external inductor, which simplifies the design process, improves the driver reliability, and reduces cost.

The LED driver adjusts the current using a shunt resistor and a switching circuitry that works at a frequency high enough to avoid flickering, and dimming can be managed by using pulse-width modulation (PWM) to set the duty cycle between 0 % and 100 %. For high speed PWM dimming, the best way to accomplish this is using a fast MOSFET in parallel with the LED chain as shown in figure 1 (a) (see the MOSFET named Q1).

Finally, the signal coming out from the Tx microcontroller, uses a training sequence with “ones” and “zeroes” for synchronization purposes to detect the starting frame of every message. And the message is also made of a large sequence of “ones” and “zeroes”. Those “ones” and “zeroes” reach the fast MOSFET, which will allow (for “ones”) or not (for “zeroes”) the current flow through the LEDs.

2.2. Receiver characteristics

After the optical signal has been electronically recovered by the photodiode it must be converted into a voltage drop and amplified in order to improve the Signal-to-Noise Ratio (SNR). When using high impedance setups, the thermal noise is reduced at the expense of a low sensitivity. A Transimpedance Amplifier (TIA) may enlarge the system sensitivity while keeping a low thermal noise level and, at the same time, amplify the signal level between 10 dB and 20 dB generating an output voltage drop. In this project it has been used a MAX3665 TIA, which gives a differential output voltage drop (differential signals also reduce the noise level). The TIA includes a low pass filter to amplify the SNR and also to perform frequency selection in the range of interest below 660 MHz. Also, great care must be taken when designing the paths in this stage with the following one, as they must be 50 Ω impedance matching conditions in order to avoid signal attenuations due to reflection effects.

Once the SNR has been improved it is time to synchronize the bit transmission with a clock signal in order to make it easier to detect every single bit. As a result, the Clock-Recovery and Data Retiming chip MAX3676 gives an output with two differential signals to reduce the noise level: The first one is the data stream and the second one is a clock signal synchronized with the data stream. In this case it is easy to know when every measurement must be done. In general, measurements must be done with every interruption detected in the clock signal. This serializer

chip also contains a previous limiting amplifier to protect the chip itself. Again, the circuit paths must be designed with 50Ω impedance to reduce reflection effects.

A further deserializer is introduced in the receiver in order to convert the serial data stream coming from the previous stage into a parallelized data stream of 8 bits (1 byte) per pulse, which is very useful to improve the data transmission speed. Besides, this deserializer also digitalizes the signal to improve its quality and it also produces a new clock signal synchronized with the new parallelized data (i.e. every interruption takes place when every byte is sent). In this way the microcontroller captures data in parallel.

The Firmware running in the microcontroller is used in order to recover every digitalized byte and to control the clock signal at the output of the deserializer.

III. Bit Error Rate (BER) and Quality factor (Q)

It is well known that the maximum acceptable rate of errors in a communication link must be in the order of 1 erroneous bit every 1000 transmitted bits. This is the concept behind the parameter called Bit Error Rate (BER), which is normalized to 1. It means that 1 error per 1000 transmitted bits corresponds to a $BER = 10^{-3}$. The acceptable limit in a VLC system is in this order, which means that the BER limit is defined as $BER \sim 10^{-3}$.

In our prototype a Digital InfiniiVision 6000 X-Series Oscilloscope Agilent was used to measure the quality of the signal through the Quality Factor (Q-factor). This parameter gives a notion of the mixture of arriving “ones” and “zeros”. It is based on measuring the height (voltage) of every arriving bit. Then it calculates the mean voltage value of the “ones” (μ_1), the mean voltage value of the “zeros” (μ_0), the standard deviation of the “ones” (σ_1), and the standard deviation of the “zeros” (σ_0). See figure 5.

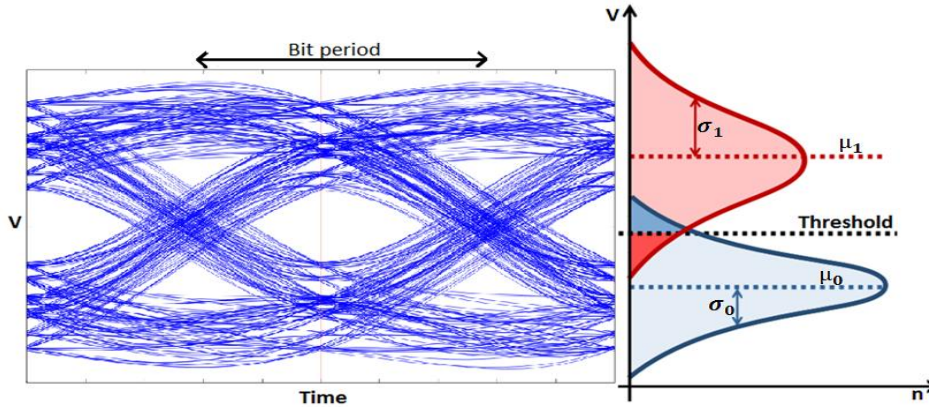


Figure 5. Eye pattern of a large number of bits (left); and corresponding number of arriving bits (n) vs. the voltage level (V) (right). This figure depicts the mean value (μ) and standard deviation (σ) for the bits “ones” (red) and the bits “zeroes” (blue).

When these parameters are measured, it is possible to acquire very easily the Q-factor from them like this [21]:

$$Q = \frac{\mu_1 - \mu_0}{\sigma_1 + \sigma_0} \quad (3.1)$$

Which is even more interesting is that this Q-factor can be related univocally with the BER factor like this [21]:

$$BER = \frac{1}{2} \cdot \operatorname{erfc} \left(\frac{Q}{\sqrt{2}} \right) \quad (3.2)$$

Here there is a method to obtain the BER from the Q-factor, which may be measured by an oscilloscope. It must be noticed that none of them have got dimensions.

In the frame of this project, as an acceptable link must have a **BER strictly below 10^{-2}** (in the order of 10^{-3}), it means that the **Q-factor value must be strictly above the value “2.32”**.

IV. Results

The hardware designed in this project showed its possibility to establish a strong communication link using visible light LEDs, but three further experiments were developed to define the real capabilities of this setup: Maximum distance it may support at a considerable high speed of 700 kb/s, maximum speed it may afford at a distance of 2 meters (typical distance between the roof and a table in a room), and maximum incidence angle it may sustain with a speed of 700 kb/s and at 2 meters distance. Those maximum values are defined for the acceptance limit given in section III, and, furthermore, all measurements are statistically treated with a mean value of up to 50 measurements.

3.1. Maximum distance characterization

Table 3 shows the Q-factor (and equivalent BER) measured for changing distances when the bit rate is 700 kb/s and there is a normal incidence between the transmitting LEDs and the photodiode in the receiver.

Table 3. Q-factor (and BER in parenthesis) for all six LED emitters when changing distances with a constant bit rate of 700 kb/s.

Distance, d (m)	LED1 (R)	LED2 (G)	LED3 (B)	LED4 (HW)	LED5 (NW)	LED6 (CW)
1	7.654 ($9.741 \cdot 10^{-15}$)	7.435 ($5.228 \cdot 10^{-14}$)	7.635 ($1.129 \cdot 10^{-14}$)	7.535 ($2.442 \cdot 10^{-14}$)	7.517 ($2.802 \cdot 10^{-14}$)	4.655 ($1.620 \cdot 10^{-6}$)
2	6.864 ($3.348 \cdot 10^{-12}$)	6.156 ($3.730 \cdot 10^{-10}$)	6.171 ($3.393 \cdot 10^{-10}$)	6.761 ($6.852 \cdot 10^{-12}$)	7.197 ($3.078 \cdot 10^{-13}$)	3.477 ($2.535 \cdot 10^{-4}$)
3	5.970 ($1.186 \cdot 10^{-9}$)	4.716 ($1.203 \cdot 10^{-6}$)	5.195 ($1.024 \cdot 10^{-7}$)	5.887 ($1.966 \cdot 10^{-9}$)	6.215 ($2.566 \cdot 10^{-10}$)	1.914 ($2.780 \cdot 10^{-2}$)
4	5.368 ($3.981 \cdot 10^{-8}$)	2.920 ($1.800 \cdot 10^{-3}$)	3.987 ($3.346 \cdot 10^{-5}$)	5.017 ($2.624 \cdot 10^{-7}$)	5.253 ($7.482 \cdot 10^{-8}$)	-
5	4.785 ($8.549 \cdot 10^{-7}$)	-	3.098 ($9.742 \cdot 10^{-4}$)	4.175 ($1.490 \cdot 10^{-5}$)	4.660 ($1.581 \cdot 10^{-6}$)	-
6	3.997 ($3.208 \cdot 10^{-5}$)	-	1.950 ($2.560 \cdot 10^{-2}$)	3.074 ($1.100 \cdot 10^{-3}$)	3.816 ($6.782 \cdot 10^{-5}$)	-
7	3.385 ($3.559 \cdot 10^{-4}$)	-	-	2.554 ($5.300 \cdot 10^{-3}$)	3.307 ($4.715 \cdot 10^{-4}$)	-
8	2.612 ($4.500 \cdot 10^{-3}$)	-	-	-	2.319 ($1.020 \cdot 10^{-2}$)	-

The data in table 3 are represented below in figure 6, as the Q-factor vs. distance and channel.

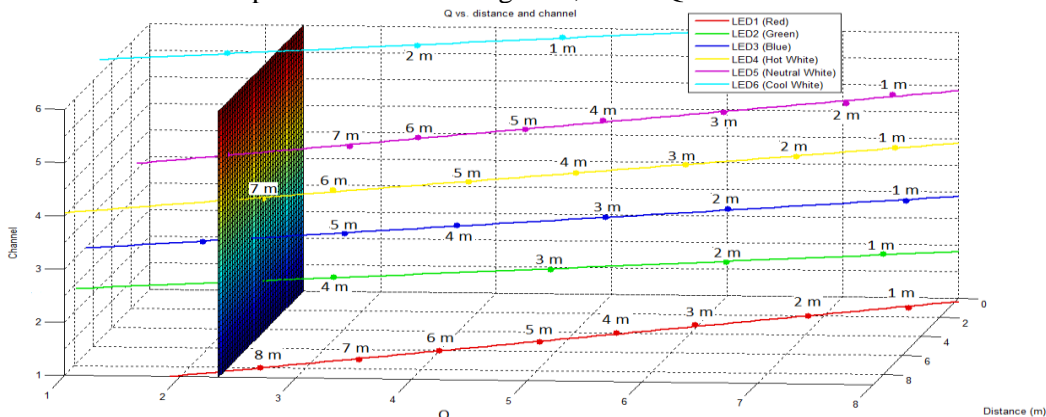


Figure 6. Q-factor vs. distance and channel. The coloured plane on the left side represents the acceptable limit ($Q = 2.32$), which means that all the points on its left side correspond to non-acceptable links.

The measured data seem to approximate well to straight lines in this experiment.

The main problem in this case was the lack of illuminance at the receiver side. It could be tested that the illumination achieved in the receiver side for the last valid measurement of every

channel was, in general, around only a 10 % over the background illumination. It means that if more powerful LEDs were used it seems quite probable that those distances could be even improved.

3.2. Maximum data rate characterization

Table 4 shows the Q-factor (and equivalent BER) measured for changing data rates when the distance is 2 meters and there is a normal incidence between the transmitting LEDs and the photodiode in the receiver.

Table 4. Q-factor (and BER in parenthesis) for all six LED emitters when changing data rates with a constant distance of 2 meters.

Data Rate (Mbps)	LED1 (R)	LED2 (G)	LED3 (B)	LED4 (HW)	LED5 (NW)	LED6 (CW)
0.5	7.828 ($2.478 \cdot 10^{-15}$)	6.508 ($3.808 \cdot 10^{-11}$)	7.867 ($1.816 \cdot 10^{-15}$)	7.842 ($2.217 \cdot 10^{-15}$)	7.828 ($2.478 \cdot 10^{-15}$)	6.840 ($3.960 \cdot 10^{-12}$)
1	5.947 ($1.366 \cdot 10^{-9}$)	4.675 ($1.470 \cdot 10^{-6}$)	5.930 ($1.515 \cdot 10^{-9}$)	5.948 ($1.357 \cdot 10^{-9}$)	6.228 ($2.362 \cdot 10^{-10}$)	4.955 ($3.617 \cdot 10^{-7}$)
1.5	4.888 ($5.093 \cdot 10^{-7}$)	3.688 ($1.130 \cdot 10^{-4}$)	4.824 ($7.035 \cdot 10^{-7}$)	4.942 ($3.866 \cdot 10^{-7}$)	5.264 ($7.048 \cdot 10^{-8}$)	4.142 ($1.721 \cdot 10^{-5}$)
2	4.328 ($7.523 \cdot 10^{-6}$)	3.128 ($8.800 \cdot 10^{-4}$)	4.316 ($7.944 \cdot 10^{-6}$)	4.350 ($6.807 \cdot 10^{-6}$)	4.344 ($6.996 \cdot 10^{-6}$)	3.291 ($4.992 \cdot 10^{-4}$)
2.5	3.893 ($4.951 \cdot 10^{-5}$)	2.532 ($5.671 \cdot 10^{-3}$)	3.904 ($4.731 \cdot 10^{-5}$)	3.816 ($6.782 \cdot 10^{-5}$)	3.923 ($4.373 \cdot 10^{-5}$)	2.542 ($5.511 \cdot 10^{-3}$)
3	3.278 ($5.227 \cdot 10^{-4}$)	-	3.306 ($4.732 \cdot 10^{-4}$)	3.305 ($4.749 \cdot 10^{-4}$)	3.317 ($4.549 \cdot 10^{-4}$)	-
3.5	3.067 ($1.081 \cdot 10^{-3}$)	-	3.064 ($1.092 \cdot 10^{-3}$)	3.076 ($1.049 \cdot 10^{-3}$)	3.082 ($1.028 \cdot 10^{-3}$)	-
4	2.461 ($6.928 \cdot 10^{-3}$)	-	2.858 ($2.132 \cdot 10^{-3}$)	2.551 ($5.371 \cdot 10^{-3}$)	2.491 ($6.369 \cdot 10^{-3}$)	-
4.5	-	-	2.523 ($5.818 \cdot 10^{-3}$)	-	-	-

The data in table 4 are represented below in figure 7, as the Q-factor vs. data rate and channel.

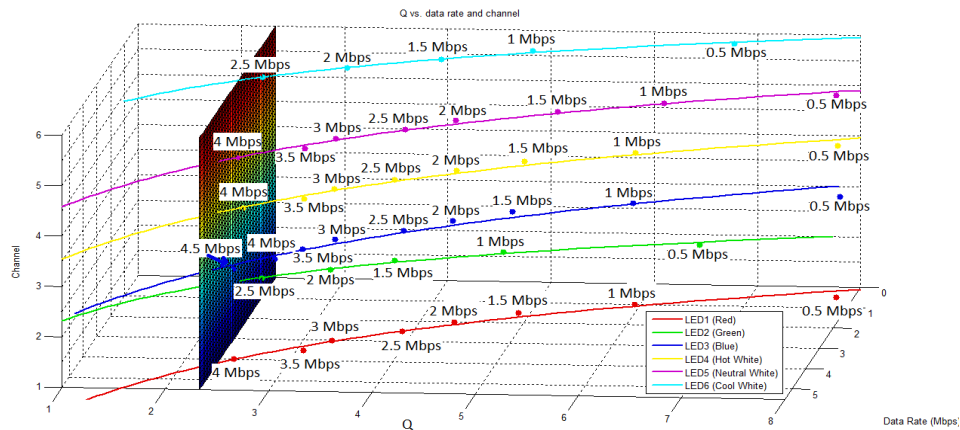


Figure 7. Q-factor vs. data rate and channel. The coloured plane on the left side represents the acceptable limit ($Q = 2.32$), which means that all the points on its left side correspond to non-acceptable links.

In this experiment the measured data seem to approximate well to exponential curves.

The main problem in this case was the fact that LEDs are attenuated in intensity when the modulation speed increases, so that at the end they seem to shut down. And then, when they shut down the Q-factor decreases very fast. This is an effect different from dimming. While dimming can be used to attenuate the intensity changing the duty cycle for comfort purposes, in this case LEDs seem to attenuate because they cannot support such high speeds because of their response times, which become larger than the bit period at high speeds.

3.3. Maximum incidence angle characterization

Table 5 shows the Q-factor (and BER) measured for changing incident angles between the transmitting LEDs and the receiver when the distance is 2 meters and the data rate is 700 kbps.

Table 5. Q-factor (and BER in parenthesis) for all six LED emitters when changing angles with a constant distance of 2 meters and a constant data rate of 700 kbps.

Incidence angle (°)	LED1 (R)	LED2 (G)	LED3 (B)	LED4 (HW)	LED5 (NW)	LED6 (CW)
0	7.302 ($1.418 \cdot 10^{-13}$)	4.446 ($4.374 \cdot 10^{-6}$)	6.783 ($5.885 \cdot 10^{-12}$)	7.353 ($9.690 \cdot 10^{-14}$)	7.446 ($4.811 \cdot 10^{-14}$)	7.435 ($5.228 \cdot 10^{-14}$)
15	6.917 ($2.307 \cdot 10^{-12}$)	4.298 ($8.617 \cdot 10^{-6}$)	6.602 ($2.028 \cdot 10^{-11}$)	6.879 ($3.014 \cdot 10^{-12}$)	7.201 ($2.989 \cdot 10^{-13}$)	7.322 ($1.222 \cdot 10^{-13}$)
30	6.697 ($1.064 \cdot 10^{-11}$)	4.067 ($2.381 \cdot 10^{-5}$)	6.398 ($7.871 \cdot 10^{-11}$)	5.726 ($5.141 \cdot 10^{-9}$)	6.009 ($9.334 \cdot 10^{-10}$)	7.063 ($8.147 \cdot 10^{-13}$)
45	5.724 ($5.202 \cdot 10^{-9}$)	3.511 ($2.232 \cdot 10^{-4}$)	5.818 ($2.978 \cdot 10^{-9}$)	2.848 ($2.200 \cdot 10^{-3}$)	3.360 ($3.897 \cdot 10^{-4}$)	5.971 ($1.179 \cdot 10^{-9}$)
60	4.680 ($1.434 \cdot 10^{-6}$)	2.423 ($7.696 \cdot 10^{-3}$)	5.119 ($1.536 \cdot 10^{-7}$)	-	-	3.109 ($9.386 \cdot 10^{-4}$)
75	1.872 ($3.060 \cdot 10^{-2}$)	1.003 ($1.579 \cdot 10^{-1}$)	2.652 ($4.001 \cdot 10^{-3}$)	-	-	-

The data in table 5 are represented below in figure 8, as the Q-factor vs. angle and channel.

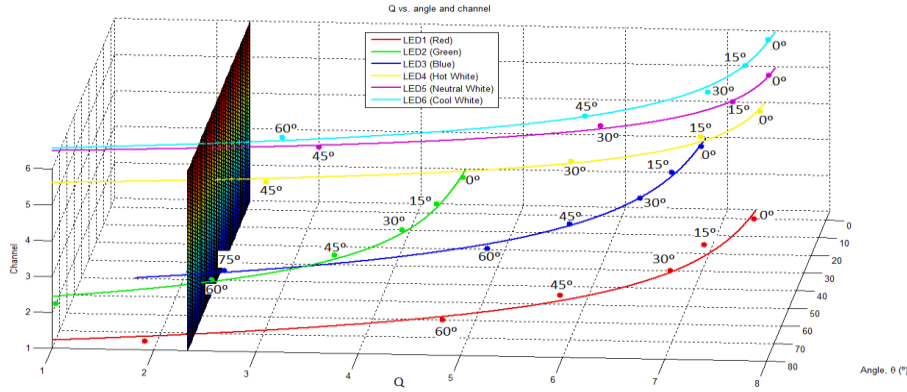


Figure 8. Q-factor vs. angle and channel. The coloured plane on the left side represents the acceptable limit ($Q = 2.32$), which means that all the points on its left side correspond to non-acceptable links.

In this experiment the measured data seem to approximate well to exponential curves (of the type " $C - a \cdot e^{-bx}$ ", where C , a and b are constants).

V. Conclusions

A Visible Light Communication (VLC) link showing a considerably high potential for practical indoor applications has been developed. This practical system achieves large distances (up to 8 meters at 700 kbps), considerably high transmission speeds (up to 4.5 Mbps at 2 meters) and high angle apertures (up to 75° at 700 kbps and 2 meters). Besides, this system contains interchangeable LED emitters for spectrally tunable VLC systems, which contains several stages to improve the SNR and detect information with inexpensive components. This way it becomes a real and practical solution for future Visible Light Communications (VLC). Our main conclusions are:

First, this link has achieved good performances in distance: Up to 8 meters with a considerably high data rate of 700 kbps, which could be even improved if more powerful LEDs or a larger number of LEDs per channel were used (as the driver might support up to 75 V if desired), as the main problem to reach larger distances is that their illumination is very low. It was not enough for even illuminate properly with at least 500 lx (according to the ISO 12464-1 standard) a table at a distance of two meters from the roof. Therefore, further improvements can be achieved with more powerful LEDs or a larger number of them, using the same transmitter and receiver. Another way to improve the results could rely on changing the driver

configuration to provide a larger constant current, but this is often linked to the use of more powerful LEDs anyway.

Second, it has also shown high speed links (up to 4.5 Mbps) in a very practical case in which the link distance is of 2 meters (typical distance from roof to tables). In this case, further improvements could be also achieved if other LEDs with faster response (lower response times) were used, as in this case all LEDs become dark when they are modulated very fast, so they seem to shut down. It means that if some other kind of LEDs more resistant to high speed modulations (lower response time) were used, better results could be probably achieved.

Third, it has also shown its capability to provide a communication link in considerably broad apertures (up to 75°) in a very practical case in which the link distance is of 2 meters (typical distance from roof to tables) and the transmission speed is considerably high (700 kbps). And perhaps, even further improvements in aperture might be achieved if fisheye lenses were used in front of the photodiode.

Note

A video of the performance of the setup may be seen in the following link: https://youtu.be/Gu_6ZUbHBU0

Acknowledgments

I would like to thank Jorge E. Higuera, F. Javier Campoy, Carles Ricart, María S. Millán, Diana and my family a lot.

References

- [1] M. Perálvarez, J. Higuera, W. Hertog, Ó. Motto, J. Carreras, "Solid-state lighting: an approach to energy-efficient illumination. Materials for sustainable energy applications: Conversion, storage, transmission and consumption", Ed. Pan Stanford Publishing ISBN 9789814411813, pp. 693-750, Barcelona, Spain, 2016.
- [2] N. Chi, H. Haas, M. Kavehrad, T. D. C. Little, X.L. Huang, "Visible Light Communications: Demand Factors, Benefits and Opportunities", IEEE Wireless Communications, Ed. Guest, Apr. 2015.
- [3] S. Dimitrov, H. Haas, "Principles of LED light communications: towards networked Li-Fi", Ed. Cambridge University Press, United Kingdom, 2015.
- [4] G. Cossu, A. M. Khalid, P. Choudhury, R. Corsini, E. Ciaramella, "3.4 gbit/s visible optical wireless transmission based on RGB LED," *Opt. Exp.*, vol. 20, no. 26, pp. B501–B506, Dec. 2012.
- [5] D. Tsonev et al., "A 3 Gb/s Single LED OFDM-Based Wireless VLC Link Using a Gallium Nitride μ -LED", IEEE Photon. Technol. Lett., vol. 26, no. 7, pp. 637-640, Apr. 2014.
- [6] F.-M. Wu et al., "3.22-gb/s WDM visible light communication of a single RGB LED employing carrier-less amplitude and phase modulation", in Proc. OFC/NFOEC, Anaheim, CA, USA, 2013, pp. 1-3.
- [7] Y. Wang, N. Chi, J. Yu, H. Shang, "Demonstration of 575-mb/s downlink and 225-mb/s uplink bi-directional SCM-WDM visible light communication using RGB LED and phosphor-based LED", *Opt. Exp.*, vol. 21, no. 1, pp. 1203-1208, Jan., 2013.
- [8] N. Fujimoto, H. Mochizuki, "477 mbit/s visible light transmission based on OOK-NRZ modulation using a single commercially available visible LED and a practical LED driver with a pre-emphasis circuit", in Proc. OFC/NFOEC, Anaheim, CA, USA, 2013, pp. 1-3.
- [9] C. Kottke, J. Hilt, K. Habel, J. Vucic, K.-D. Langer, "1.25 gbit/s visible light WDM link based on dmt modulation of a single RGB LED luminary", in Proc. 38th ECOC, Amsterdam, The Netherlands, 2012, pp. 1-3.
- [10] G. Cossu, A. M. Khalid, P. Choudhury, R. Corsini, E. Ciaramella, "2.1 gbit/s visible optical wireless transmission", in Proc. ECOC, Amsterdam, The Netherlands, 2012, pp. 1-4.
- [11] A. Azhar, T. Tran, D. O'Brien, "A Gigabit/s Indoor Wireless Transmission Using MIMO-OFDM Visible-Light Communications", IEEE Photon. Technol. Lett., vol. 25, no. 2, pp. 171-174, Jan., 2013.
- [12] A. M. Khalid, G. Cossu, R. Corsini, P. Choudhury, E. Ciaramella, "1-Gb/s Transmission Over a Phosphorescent White LED by Using Rate-Adaptive Discrete Multitone Modulation", IEEE Photon. Journal, vol. 4, no. 5, Oct. 2012.
- [13] H. Li, X. Chen, B. Huang, D. Tang, H. Chen, "High bandwidth visible light communications based on a post-equalization circuit", IEEE Photon. Technol. Lett., vol. 26, no. 2, pp. 119-122, Jan. 2014.
- [14] S. Rajbhandari, P. Haigh, Z. Ghassemlooy, W. Popoola, "Wavelet-neural network VLC receiver in the presence of artificial light interference", IEEE Photon. Technol. Lett., vol. 25, no. 15, pp. 1424-1427, Aug. 2013.
- [15] Y. Liu, C. Yeh, Y. Wang, C. Chow, "Employing NRZI code for reducing background noise in LED visible light communication", in Proc. 18th OECC/OECC/PS, Kyoto, Japan, 2013, pp. 1-2.
- [16] H.-S. Kim, D.-R. Kim, S.-H. Yang, Y.-H. Son, S.-K. Han, "Single side-band orthogonal frequency division multiplexing signal transmission in rf carrier allocated visible light communication", IET Optoelectron., vol. 7, no. 6, pp. 125-130, Dec. 2013.
- [17] L. Fan, L. Ding, F. Liu, Y. Wang, "Design of wireless optical access system using LED based android mobile", in Proc. Int. Conf. WCSP, pp. 1-4, Hangzhou, China, 2013.
- [18] A. H. Azhar, T. Tuan-Anh, D. O'Brien, "Demonstration of high-speed data transmission using mimo-ofdm visible light communications", in Proc. IEEE GC Wkshps, FL, pp. 1052-1056, Miami, USA, 2010.
- [19] P. Haigh, Z. Ghassemlooy, S. Rajbhandari, I. Papakonstantinou, "Visible Light Communications Using Organic Light Emitting Diodes", IEEE Communications Magazine, vol. 51, no. 8, pp. 148-154, Aug. 2013.
- [20] P. Haigh, Z. Ghassemlooy, I. Papakonstantinou, "1.4-mb/s white organic LED transmission system using discrete multitone modulation", IEEE Photon. Technol. Lett., vol. 25, no. 6, pp. 615-618, Mar. 2013.
- [21] J. M. Gené, J. A. Lázaro, "Receivers", Classnotes, Fibers and Telecommunications subject, Master in Photonics, Departament de Teoria del Senyal i Comunicacions, Escola Tècnica Superior d'Enginyeria de Telecomunicació de Barcelona, UPC.